NIH Public Access
Author Manuscript
Nature. Author manuscript; available in PMC 2011 May 10.

Published in final edited form as:
Nature. 2007 December 20; 450(7173): 1235–1239. doi:10.1038/nature06385.

Isolation of rare circulating tumour cells in cancer patients by microchip technology

Sunitha Nagrath[1,*], **Lecia V. Sequist**[2,*], **Shyamala Maheswaran**[2], **Daphne W. Bell**[2,†], **Daniel Irimia**[1], **Lindsey Ulkus**[2], **Matthew R. Smith**[2], **Eunice L. Kwak**[2], **Subba Digumarthy**[2], **Alona Muzikansky**[2], **Paula Ryan**[2], **Ulysses J. Balis**[1,†], **Ronald G. Tompkins**[1], **Daniel A. Haber**[2], and **Mehmet Toner**[1]

[1]Surgical Services and BioMEMS Resource Center, Massachusetts General Hospital, Harvard Medical School, and Shriners Hospital for Children, Boston, Massachusetts 02114, USA

[2]Massachusetts General Hospital Cancer Center, Harvard Medical School, Boston, Massachusetts 02114, USA

Abstract

Viable tumour-derived epithelial cells (circulating tumour cells or CTCs) have been identified in peripheral blood from cancer patients and are probably the origin of intractable metastatic disease[1–4]. Although extremely rare, CTCs represent a potential alternative to invasive biopsies as a source of tumour tissue for the detection, characterization and monitoring of non-haematologic cancers[5–8]. The ability to identify, isolate, propagate and molecularly characterize CTC subpopulations could further the discovery of cancer stem cell biomarkers and expand the understanding of the biology of metastasis. Current strategies for isolating CTCs are limited to complex analytic approaches that generate very low yield and purity[9]. Here we describe the development of a unique microfluidic platform (the 'CTC-chip') capable of efficient and selective separation of viable CTCs from peripheral whole blood samples, mediated by the interaction of target CTCs with antibody (EpCAM)-coated microposts under precisely controlled laminar flow conditions, and without requisite pre-labelling or processing of samples. The CTC-chip successfully identified CTCs in the peripheral blood of patients with metastatic lung, prostate, pancreatic, breast and colon cancer in 115 of 116 (99%) samples, with a range of 5–1,281 CTCs per ml and approximately 50% purity. In addition, CTCs were isolated in 7/7 patients with early-stage prostate cancer. Given the high sensitivity and specificity of the CTC-chip, we tested its potential utility in monitoring response to anti-cancer therapy. In a small cohort of patients with metastatic cancer undergoing systemic treatment, temporal changes in CTC numbers correlated reasonably well with the clinical course of disease as measured by standard radiographic methods. Thus, the CTC-chip provides a new and effective tool for accurate identification and measurement of CTCs in patients with cancer. It has broad implications in advancing both cancer biology

Correspondence and requests for materials should be addressed to M.T. (mtoner@hms.harvard.edu).
†Present addresses: National Human Genome Research Institute/NIH Cancer Genetics Branch, Bethesda, Maryland 20892, USA (D.W.B.); Department of Pathology, University of Michigan Health System, Ann Arbor, Michigan 48109, USA (U.J.B.).
*These authors contributed equally to this paper.

Full Methods and any associated references are available in the online version of the paper at www.nature.com/nature. Supplementary Information is linked to the online version of the paper at www.nature.com/nature.

Author Contributions S.N., L.V.S., R.G.T., D.A.H. and M.T. designed and conducted the study. S.M., D.W.B. and L.U. performed gene expression analyses; D.I. contributed to the microfluidic system. M.R.S., E.L.K. and P.R. acquired clinical samples. U.J.B. provided input on cytopathology; A.M. performed statistical analysis; and S.D. performed radiology measurements. S.N., L.V.S., D.W.B., S.M., D.I., D.A.H. and M.T. participated in data analysis and writing of the manuscript.

Author Information Reprints and permissions information is available at www.nature.com/reprints. The authors declare competing financial interests: details accompany the full-text HTML version of the paper at www.nature.com/nature.

NIH-PA Author Manuscript
NIH-PA Author Manuscript
NIH-PA Author Manuscript

NIH-PA Author Manuscript

NIH-PA Author Manuscript

NIH-PA Author Manuscript

research and clinical cancer management, including the detection, diagnosis and monitoring of cancer[10].

CTCs are rare, comprising as few as one cell per 10^9 haematologic cells in the blood of patients with metastatic cancer, hence their isolation presents a tremendous technical challenge[7,9,11–13]. Microfluidic lab-on-a-chip devices provide unique opportunities for cell sorting and rare-cell detection; they have been successfully used for microfluidic flow cytometry[14], continuous size-based separation[15,16] and chromatographic separation[17]. Despite their success in manipulating microlitre amounts of simple liquids in microscale channels[14,18,19], they have thus far shown limited capability to deal with the cellular and fluid complexity of large volumes (millilitres) of whole blood samples[20–22].

Here we describe the development and application of a microfluidic device (the 'CTC-chip') that can efficiently and reproducibly isolate CTCs from the blood of patients with common epithelial tumours (Fig. 1, and Supplementary Fig. 1). The CTC-chip (Fig. 1b) consists of an array of microposts (Supplementary Fig. 1c) that are made chemically functional with anti-epithelial-cell-adhesion-molecule (EpCAM, also known as TACSTD1) antibodies. Anti-EpCAM provides the specificity for CTC capture from unfractionated blood because EpCAM is frequently overexpressed by carcinomas of lung, colorectal, breast, prostate, head and neck, and hepatic origin, and is absent from haematologic cells[23,24].

Two essential parameters that determine the efficiency of cell capture on the CTC-chip are: (1) flow velocity, because it influences the duration of cell–micropost contact; and (2) shear force, which must be sufficiently low to ensure maximum cell–micropost attachment. To optimize these parameters we employed theoretical analyses characterizing the interaction of cells with microposts distributed within the flow path (Supplementary Figs 1c and 2). Briefly, the simulation indicated an equilateral triangular arrangement, with a 50 μm distance between microposts and a 50 μm shift after every 3 rows, to be the most efficient geometric arrangement. For a given volumetric flow rate of 1 ml h^{-1} through the device, the maximum shear stress experienced by a cell near the micropost surface was estimated to be 0.4 dyn cm^{-2} at θ =68° and the expected maximum velocity was 460 μm s^{-1} (Supplementary Fig. 2b–d), within the range facilitating maximum cell attachment according to linear shear stress chamber studies (Supplementary Fig. 3). On the basis of the simulation results, we fabricated a CTC-chip containing an array of 78,000 microposts within a 970mm^2 surface.

To determine the efficiency of capture, we spiked non-small-cell lung cancer (NSCLC) cells (NCI-H1650) into phosphate buffered saline (PBS) at 100 cells ml^{-1} and captured the spiked cancer cells using the CTC-chip. NSCLC cells were visually evident about EpCAM-coated microposts, whereas no cancer cells were seen following flow through uncoated posts (Supplementary Fig. 4a–c). The calculated capture efficiency was 65% and decreased significantly at flow rates above 2.5 ml h^{-1} (Fig. 2a), presumably owing to increased shear stress, consistent with our simulation predictions. The efficiency of capture was not enhanced at flow rates less than 0.75 ml h^{-1}, leading us to select a flow rate of 1–2 ml h^{-1} for subsequent studies.

To determine the effect of cellular EpCAM expression on efficiency of CTC capture, we compared capture rates among cancer cell lines with varied EpCAM expression, including NSCLC NCI-H1650 cells and breast cancer SKBr-3 cells, with >500,000 antigens per cell; prostate cancer PC3-9 cells, with approximately 50,000 antigens per cell; and bladder cancer T-24 cells, with approximately 2,000 antigens per cell[25]. Each cell line was spiked into PBS at a concentration of 100 cells ml^{-1} and analysed, resulting in a mean capture yield of >65% in all cases (Fig. 2b). Interestingly T-24 cells with relatively low EpCAM expression were

NIH-PA Author Manuscript

NIH-PA Author Manuscript

NIH-PA Author Manuscript

captured as efficiently as high-level antigen-expressing cells. We believe this is due to the augmented cell–substrate interactions inherent within the CTC-chip.

To evaluate cell capture under more physiological conditions, we conducted a series of experiments in which NCI-H1650 cells were spiked into whole blood from healthy donors. Suspensions at concentrations ranging from 50 to 50,000 tumour cells per ml of whole blood were analysed, yielding recovery rates of >60% in all cases (Fig. 2c). To assess the potential steric hindrance of red blood cells in the flow path, these studies were repeated using lysed blood from healthy donors. Capture rates were comparable under both conditions (r^2 = 0.99; Fig. 2c). Similar results were obtained using whole blood and lysed samples from NSCLC patients (Supplementary Fig. 4d, e). We thus concluded that the CTC-chip does not require blood-sample pre-processing.

Having optimized the CTC-chip with controlled quantities of cancer-derived cells, we tested its capacity to capture CTCs from whole blood samples donated by cancer patients. A total of 116 samples from 68 patients with epithelial cancers including NSCLC (*n* = 55), prostate (*n* = 26), pancreatic (*n* = 15), breast (*n* = 10) and colon (*n* = 10) were studied. The majority of patients had metastatic disease; however, 7 of 26 subjects with prostate cancer had untreated, clinically localized disease with specimens collected before prostatectomy with curative intent (Supplementary Table 2). The average volume of blood analysed was 2.7 ml per sample (range, 0.9 to 5.1 ml). We also examined samples from 20 healthy individuals (3.0 ± 0.4 ml (mean ± s.d.) of blood per subject) as controls (Supplementary Table 1).

CTCs captured from a group of patient samples were identified using a comprehensive image analysis algorithm, consisting of staining with 4,6-diamidino-2-phenylindole (DAPI) for DNA content, and using rhodamine-conjugated anti-cytokeratin (also known as KERSMCR) antibodies for epithelial cells, and fluorescein-conjugated anti-CD45 antibodies for haematologic cells (Fig. 2d–k, and Supplementary Fig. 5). Cells captured by anti-EpCAM-coated microposts and staining for cytokeratin were scored as CTCs, whereas CD45-positive cells were scored as contaminating normal haematologic cells. The morphologic characteristics exhibited by the captured CTCs were consistent with malignant cells, including large cellular size with high nuclear:cytoplasmic ratios and visible nucleoli (Fig. 2d–g). The mean viability of captured cells was 98.5 ± 2.3% (mean ± s.d.), determined by assessing cell membrane integrity in 10 high-power fields of view per CTC-chip in 4 samples obtained from lung (*n* = 2) and prostate (*n* = 2) cancer patients.

CTCs were identified in 115 of 116 (>99%) patient samples analysed, with the single negative specimen being a small volume sample (0.9 ml) from a patient with colorectal cancer. The number of CTCs isolated ranged from 5 to 1,281 per ml for NSCLC (155 ± 236 (mean ± s.d.) CTCs per ml), 16 to 292 (86 ± 78) for metastatic prostate, 25 to 174 (94 ± 63) among localized prostate cancers, 9 to 831 (196 ± 228) for pancreatic, 5 to 176 (79 ± 52) for breast, and 42 to 375 (121 ± 127) for colorectal cancers (Fig. 3a, b). The identification of CTCs in subjects with clinically localized prostate cancer at numbers approximating those in metastatic prostate cancer patients is a novel finding enabled by the high sensitivity of our technique and warrants further study. The average purity of capture, as defined by the ratio of cytokeratin$^+$ to CD45$^+$ cells, was 52% in NSCLC, 49% in metastatic prostate, 53% in localized prostate, 53% in pancreatic, 60% in breast, and 67% in colon cancers (Fig. 3c). None of the 20 healthy subjects had any identifiable CTCs (Supplementary Table 1). On the basis of these results we calculated the sensitivity (99.1%) and specificity (100%) of the CTC-chip across all five cancers. Finally, we evaluated the reproducibility of CTC capture using split samples and showed high experimental reproducibility (r^2= 0.98; Supplementary Fig. 4f).

NIH-PA Author Manuscript

NIH-PA Author Manuscript

NIH-PA Author Manuscript

To determine whether captured cells are suitable for subsequent molecular analyses, we tested expression of two tumour-specific markers: prostate-specific antigen (PSA; also known as KLK3) in prostate cancer and thyroid transcription factor-1 (TTF-1; also known as NKX2-1) in lung adenocarcinoma. Specific expression of these markers was evident by immunostaining (Fig. 4a, b, d, e), and confirmed by direct lysis of captured CTCs on the microchip and PCR with reverse transcription (RT–PCR) amplification of the individual transcripts (Fig. 4c, f). Considering the ~50% purity of captured viable CTCs (two orders of magnitude higher than currently available technologies)[26], the CTC-chip provides a powerful opportunity for CTC-based molecular analyses.

To demonstrate the unique clinical potential of our approach, we evaluated the ability of changes in CTC burden to predict changes in tumour volume in cancer patients undergoing anti-cancer treatments. Patients with advanced epithelial-based malignancies that were commencing a first or second line systemic treatment regimen were eligible. Blood samples were collected at baseline and during subsequent clinic visits; the exact follow-up schedule varied between patients. Computed tomograms (CT scans) were performed at baseline and at regular intervals according to standard clinical practice. For each CT scan, we calculated the sum of the unidimensional size in centimetres of all significant and measurable tumour sites, as per the RECIST standardized system[27]. All patients with baseline and at least one follow-up CTC sample and CT scan were analysed, including patients with NSCLC (n=3), colorectal (n=2), pancreatic (n=3) and oesophageal cancer (n=1) (Fig. 3d–i). The absolute number of CTCs captured did not necessarily correspond with tumour size, and may be influenced by other factors. The correlation between per cent change in CTC quantity and per cent change in tumour size, from first to last measurement, was analysed over all 9 patients and yielded a Pearson's correlation coefficient of 0.68 (P=0.03). These results from a small cohort of patients show that CTC quantity correlates reasonably well with clinical response and clinical non-response to treatment (Fig. 3d–i, and Supplementary Fig. 6), indicating that monitoring treatment response using the CTC-chip may ultimately be a powerful tool enabling accurate, early decision-making. The clinical impact of such an approach could be large, and could enable a decrease in patient exposure to toxicities from ineffective therapies and guide them towards the treatments most active against their specific tumour.

Other approaches to enrich or sort CTCs from peripheral blood have been previously published, including flow cytometry[28], immunomagnetic beads[9], high-throughput optical-imaging systems[29], and fibre optic array scanning[12]. Immunomagnetic-bead purification[1,13,30] is currently the lead technology in the clinical setting, with reported success in identifying CTCs in a portion of tested patients with lung, prostate, colon, breast and pancreatic cancer[30]. However, this approach isolates small numbers of CTCs (4 ± 24 (mean ± s.d.) per ml in lung; 11 ± 118 in breast; 10 ± 33 in prostate; and 1 ± 2 in both colorectal and pancreatic cancers)[30] with very low purity (0.01–0.1%)[26], and low yield (~20–60% of patients)[30]. The level of ‘biological noise’ associated with the low sensitivity, selectivity, and yield of magnetic-bead-based technologies is prohibitive to their capacity to monitor response to treatment in a dynamic fashion and for early cancer detection. Hence, this method has thus far demonstrated clinical utility only as a gross prognostic tool, classifying patients into high- and low-risk categories[1]. Conversely, the high sensitivity (1 target cell in 1 billion blood cells), selectivity (>47% purity), and yield (99%) of the CTC-chip makes it ideally suited for real-time monitoring of response to cancer therapy.

In addition, the CTC-chip is unique in that it sorts rare cells directly from whole blood in a single step. From a technical perspective, this is possible because the CTC-chip is the first microfluidic device that can successfully process millilitre volumes of whole blood. This contrasts with magnetic-bead-based systems[30] that require multiple ‘bulk’ semi-automated

NIH-PA Author Manuscript

NIH-PA Author Manuscript

NIH-PA Author Manuscript

preparatory steps (centrifugation, washing and incubation), resulting in loss and/or destruction of a significant proportion of the rare cells. In addition to its simplicity, the CTC-chip is readily adaptable for potential use in various clinical scenarios, including changes in throughput and in the antibody on the microposts, allowing capture of other types of rare circulating cells. The CTC-chip's one-step nature and versatility make it conducive to point-of-care use and rapid integration into clinical practice.

Finally, the CTC-chip is distinctive in that its gentle nature (maximum shear stress is 0.4 dyn cm^{-2}) allows for isolation of viable cells, whereas magnetic-bead-based approaches can only isolate fixed, non-viable cells[30]. The stationary nature of the captured cells on fixed microposts allows wash-out of non-specifically bound leukocytes, resulting in a 10^6-fold enrichment, a level of purity that is two orders of magnitude higher than existing technologies. The capacity to isolate concentrated, viable CTCs makes the CTC-chip an ideal tool for molecular access to rare CTC subpopulations such as metastatic precursor cells or cancer stem cells.

In summary, the CTC-chip captures large numbers of viable CTCs in a single step from whole blood without pre-dilution, pre-labelling, pre-fixation or any other processing steps. The techniques described here and the broader application of microfluidic rare-cell capture technology to cancer patients hold significant promise for identifying key biological determinants of blood-borne metastases, and for providing a robust platform aimed at early diagnosis and longitudinal monitoring of cancer.

Methods Summary

The microfluidic system (Fig. 1a) consists of a microfluidic chip etched in silicon (Fig. 1b), a manifold to enclose the chip (Fig. 1c, and Supplementary Fig. 1b), and a pneumatic pump (Fig. 1a) to establish the flow through the capture module (Fig. 1c). The schematic of the microfluidic system is depicted in Supplementary Fig. 1b. The dimensions of the chip are 25mm × 66 mm, with an active capture area of 19mm × 51 mm. It contains an equilateral triangular array of microposts, 100 μm tall and 100 μm in diameter with an average 50 μm gap between microposts (Supplementary Fig. 1c). For increased hydrodynamic efficiency, the repeated patterns of equilateral triangular arrays were shifted vertically by 50 μm for every three rows throughout the chip to maximize the interactions between micropost structures and cells. This array incorporates 78,000 microposts within a surface area of $970mm^2$. Microposts were fabricated with deep reactive ion etching (DRIE) by Silex. The blood specimen collection and processing, macro-to-micro coupling, identification and enumeration of CTCs, cell viability and molecular assays are described in Methods.

Supplementary Material

Refer to Web version on PubMed Central for supplementary material.

Acknowledgments

We thank A. Amin for technical assistance in running experiments, O. Hurtado for clean room work, S. Murthy for surface chemistry, L. Romonosky for cell counting, D. Hyde for digital pictures and D. Poulsen for illustrations. We are also grateful to R. Kapur and his team for technical assistance. The authors acknowledge funding from the National Institutes of Health (to M.T.), and the Doris Duke Distinguished Clinical Scientist Award (to D.A.H.).

References

1. Cristofanilli M, et al. Circulating tumor cells, disease progression, and survival in metastatic breast cancer. N Engl J Med. 2004; 351:781–791. [PubMed: 15317891]

NIH-PA Author Manuscript

NIH-PA Author Manuscript

NIH-PA Author Manuscript

2. Steeg PS. Tumor metastasis: mechanistic insights and clinical challenges. Nature Med. 2006; 12:895–904. [PubMed: 16892035]
3. Gupta GP, Massague J. Cancer metastasis: building a framework. Cell. 2006; 127:679–695. [PubMed: 17110329]
4. Reya T, Morrison SJ, Clarke MF, Weissman IL. Stem cells, cancer, and cancer stem cells. Nature. 2001; 414:105–111. [PubMed: 11689955]
5. Mocellin S, Hoon D, Ambrosi A, Nitti D, Rossi CR. The prognostic value of circulating tumor cells in patients with melanoma: a systematic review and meta-analysis. Clin Cancer Res. 2006; 12:4605–4613. [PubMed: 16899608]
6. Smerage JB, Hayes DF. The measurement and therapeutic implications of circulating tumour cells in breast cancer. Br J Cancer. 2006; 94:8–12. [PubMed: 16317435]
7. Rolle A, et al. Increase in number of circulating disseminated epithelial cells after surgery for non-small cell lung cancer monitored by MAINTRAC(R) is a predictor for relapse: A preliminary report. World J Surg Oncol. 2005; 3:18. [PubMed: 15801980]
8. Braun S, Marth C. Circulating tumor cells in metastatic breast cancer—toward individualized treatment? N Engl J Med. 2004; 351:824–826. [PubMed: 15317898]
9. Zieglschmid V, Hollmann C, Bocher O. Detection of disseminated tumor cells in peripheral blood. Crit Rev Clin Lab Sci. 2005; 42:155–196. [PubMed: 15941083]
10. Bell DW, Haber DA. A blood-based test for epidermal growth factor receptor mutations in lung cancer. Clin Cancer Res. 2006; 12:3875–3877. [PubMed: 16818680]
11. Kahn HJ, et al. Enumeration of circulating tumor cells in the blood of breast cancer patients after filtration enrichment: correlation with disease stage. Breast Cancer Res Treat. 2004; 86:237–247. [PubMed: 15567940]
12. Krivacic RT, et al. A rare-cell detector for cancer. Proc Natl Acad Sci USA. 2004; 101:10501–10504. [PubMed: 15249663]
13. Racila E, et al. Detection and characterization of carcinoma cells in the blood. Proc Natl Acad Sci USA. 1998; 95:4589–4594. [PubMed: 9539782]
14. Fu AY, Spence C, Scherer A, Arnold FH, Quake SR. A microfabricated fluorescence-activated cell sorter. Nature Biotechnol. 1999; 17:1109–1111. [PubMed: 10545919]
15. Davis JA, et al. Deterministic hydrodynamics: taking blood apart. Proc Natl Acad Sci USA. 2006; 103:14779–14784. [PubMed: 17001005]
16. Huang LR, Cox EC, Austin RH, Sturm JC. Continuous particle separation through deterministic lateral displacement. Science. 2004; 304:987–990. [PubMed: 15143275]
17. Chang WC, Lee LP, Liepmann D. Biomimetic technique for adhesion-based collection and separation of cells in a microfluidic channel. Lab Chip. 2005; 5:64–73. [PubMed: 15616742]
18. Whitesides GM. The origins and the future of microfluidics. Nature. 2006; 442:368–373. [PubMed: 16871203]
19. Hong JW, Quake SR. Integrated nanoliter systems. Nature Biotechnol. 2003; 21:1179–1183. [PubMed: 14520403]
20. Toner M, Irimia D. Blood-on-a-chip. Annu Rev Biomed Eng. 2005; 7:77–103. [PubMed: 16004567]
21. Dittrich PS, Manz A. Lab-on-a-chip: microfluidics in drug discovery. Nature Rev Drug Discov. 2006; 5:210–218. [PubMed: 16518374]
22. El-Ali J, Sorger PK, Jensen KF. Cells on chips. Nature. 2006; 442:403–411. [PubMed: 16871208]
23. Went PT, et al. Frequent EpCam protein expression in human carcinomas. Hum Pathol. 2004; 35:122–128. [PubMed: 14745734]
24. Balzar M, Winter MJ, de Boer CJ, Litvinov SV. The biology of the 17–1A antigen (Ep-CAM). J Mol Med. 1999; 77:699–712. [PubMed: 10606205]
25. Rao CG, et al. Expression of epithelial cell adhesion molecule in carcinoma cells present in blood and primary and metastatic tumors. Int J Oncol. 2005; 27:49–57. [PubMed: 15942643]
26. Smirnov DA, et al. Global gene expression profiling of circulating tumor cells. Cancer Res. 2005; 65:4993–4997. [PubMed: 15958538]

NIH-PA Author Manuscript

NIH-PA Author Manuscript

NIH-PA Author Manuscript

27. Therasse P, et al. New guidelines to evaluate the response to treatment in solid tumors. European Organization for Research and Treatment of Cancer, National Cancer Institute of the United States, National Cancer Institute of Canada. J Natl Cancer Inst. 2000; 92:205–216. [PubMed: 10655437]

28. Terstappen LW, et al. Flow cytometry–principles and feasibility in transfusion medicine. Enumeration of epithelial derived tumor cells in peripheral blood. Vox Sang. 1998; 74(suppl. 2): 269–274. [PubMed: 9704456]

29. Kraeft SK, et al. Reliable and sensitive identification of occult tumor cells using the improved rare event imaging system. Clin Cancer Res. 2004; 10:3020–3028. [PubMed: 15131038]

30. Allard WJ, et al. Tumor cells circulate in the peripheral blood of all major carcinomas but not in healthy subjects or patients with nonmalignant diseases. Clin Cancer Res. 2004; 10:6897–6904. [PubMed: 15501967]

31. Drummond JE, Tahir MI. Laminar viscous flow through regular arrays of parallel solid cylinders. Int J Multiphase Flow. 1984; 10:515–539.

32. Murthy SK, Sin A, Tompkins RG, Toner M. Effect of flow and surface conditions on human lymphocyte isolation using microfluidic chambers. Langmuir. 2004; 20:11649–11655. [PubMed: 15595794]

NIH-PA Author Manuscript
NIH-PA Author Manuscript
NIH-PA Author Manuscript

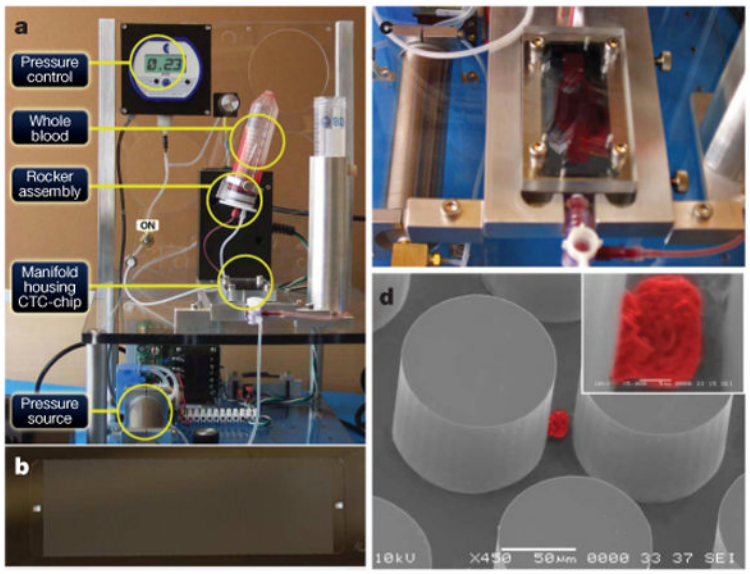

Figure 1. Isolation of CTCs from whole blood using a microfluidic device

a, The workstation setup for CTC separation. The sample is continually mixed on a rocker, and pumped through the chip using a pneumatic-pressure-regulated pump. **b**, The CTC-chip with microposts etched in silicon. **c**, Whole blood flowing through the microfluidic device. **d**, Scanning electron microscope image of a captured NCI-H1650 lung cancer cell spiked into blood (pseudo coloured red). The inset shows a high magnification view of the cell.

NIH-PA Author Manuscript

NIH-PA Author Manuscript

NIH-PA Author Manuscript

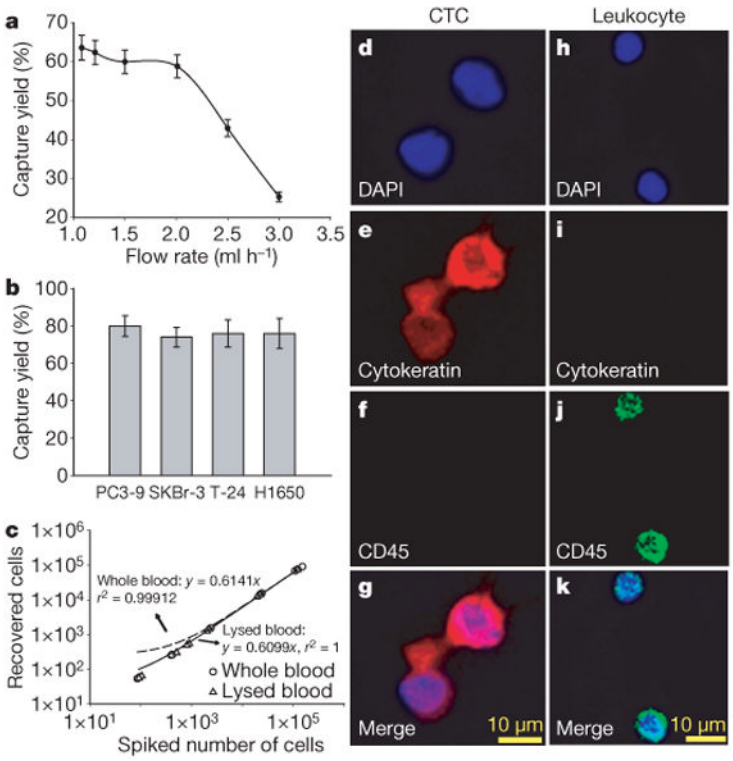

Figure 2. CTC capture and enumeration

a, Capture yield as a function of flow rate. Data shown represent measurements averaged over three devices, and each error bar represents the standard error of the mean. **b**, Capture yields from buffer spiked with 100 cells per ml of four different cell lines: prostate (PC3-9), breast (SkBr-3), bladder (T-24), and NSCLC (NCI-H1650). Each data point was repeated in at least 3 devices. The error bars represent standard deviations of measurements within each experiment. **c**, Regression analysis of capture efficiency for various target cell concentrations, comparing whole blood to lysed blood samples. The plot represents number of cells spiked versus number of cells recovered. **d**–**k**, Higher magnification (20×) images of captured CTCs and haematologic cells from NSCLC patients, stained with DAPI, and for cytokeratin and CD45. Merged images identify CTCs in panels **d**–**g** and haematologic cells in panels **h**–**k**.

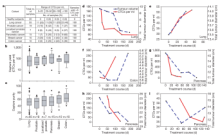

Figure 3. Enumeration of CTCs from cancer patients

a, Summary of samples and CTC counts per 1 ml of blood in patients with various advanced cancers and localized prostate cancer. **b**, Frequency of CTCs per 1 ml of blood, by diagnosis. The box plot presents the median, lower and upper quartiles (25th, 75th percentiles). Data points that lie outside the 10th and 90th percentiles are shown as outliers. **c**, Purity of captured CTCs (ratio of CTCs to total nucleated cells), by diagnosis. **d**–**i**, Serial CTC assessment. CTC quantity (red), and tumour size (blue) measured as the unidimensional sum of all significant tumour sites on a CT scan, are well correlated over the course of anti-cancer treatment for nine patients. Six of them are shown here, for whom diagnoses and specific therapies were: NSCLC, 1st-line carboplatin, paclitaxel (**d**); NSCLC, 2nd-line pemetrexed (**e**); colorectal, 1st-line 5FU, irinotecan (**f**); pancreatic, 1st-line gemcitabine, bevacizumab (**g**); pancreatic, 1st-line gemcitabine (**h**); pancreatic, 1st-line gemcitabine, erlotinib (**i**). Baseline CT scans were before therapy initiation and CTC measurements began at or shortly after the first treatment.

NIH-PA Author Manuscript NIH-PA Author Manuscript NIH-PA Author Manuscript

NIH-PA Author Manuscript
NIH-PA Author Manuscript
NIH-PA Author Manuscript

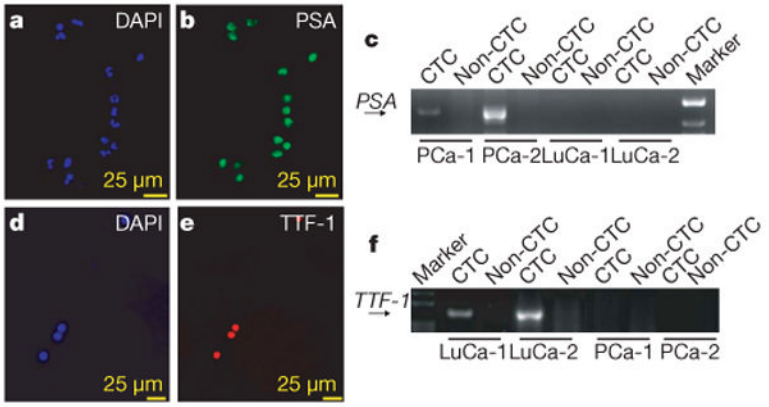

Figure 4. Characterization of CTCs with tumour-specific molecular markers

a, **b**, CTCs from a prostate cancer patient stained positive for DAPI and PSA expression. **c**, RT–PCR amplification of *PSA* transcript is seen in two patients with prostate cancer (PCa), but not in two patients with lung cancer (LuCa), and only in blood fractions enriched for CTCs as opposed to non-enriched fractions (non-CTC). **d**, **e**, CTCs from an NSCLC patient stained for DAPI and TTF-1. **f,** RT–PCR shows expression of *TTF-1* in two patients with lung cancer (LuCa), which is absent in two patients with prostate cancer (PCa), and only when RNA was eluted from blood fractions enriched for CTCs as opposed to non-enriched fractions (non-CTC).